PERGAMON

Journal of Structural Geology 24 (2002) 979–995

JOURNAL OF STRUCTURAL GEOLOGY

www.elsevier.com/locate/jstrugeo

Microstructural evolution and rheological behaviour of marbles deformed at different crustal levels

Stanislav Ulrich[a,*], Karel Schulmann[a], Martin Casey[b]

[a]*Institute of Petrology and Structural Geology, Charles University, Albertor 6, 12843 Praha 2, Czech Republic*
[b]*Department of Earth Sciences, University of Leeds, Leeds, UK*

Received 8 March 2000; revised 25 July 2001; accepted 22 August 2001

Abstract

Microstructures from naturally deformed marbles were investigated from a nappe pile with inverted Barrovian metamorphic zones. Detailed microstructural and textural work combined with existing PT data allows us to correlate microstructural types with tectonic events. Type 1 microstructure related to D1 continental underthrusting shows highly asymmetrical grain boundaries, increasing grain size and increasing intensity of lattice-preferred orientation with increasing metamorphic grade. These characteristics suggest that dislocation creep with concommitant grain boundary migration operated during the simple shear dominated underthrusting regime. Paleopiezometric and strain rate estimates show a decrease of flow stress with increasing metamorphic temperature and a strain rate of around 10^{-14} s^{-1}. Thrust related microstructure Type 2 is developed in Upper and Lower Nappes and is characterised by grain size reduction, increase of grain boundary symmetry and weaker textures. Microstructural and textural studies indicate dislocation creep with possible contribution of grain boundary sliding. Sub-grain rotation paleopiezometry and strain rate estimates show a decrease in flow stress with respect to the Type 1 microstructure and strain rate increase to around 10^{-12} to 10^{-13} s^{-1}. Type 3 microstructure is developed in thrust related shear zones in the Parautochthon and syn-convergent extensional zones in the top of the nappe pile. This microstructure shows a high contribution of diffusion creep indicating low values of flow stress and significant weakening of marble layers. The general feature of studied area is the localisation of deformation into marbles during thrusting in low metamorphic grades while in higher grades marbles are not exploited as lubricating layers.

Keywords: Marble; Microstructure; Texture; Natural deformation; Rheology

1. Introduction

Microstructural studies of naturally and experimentally deformed marbles have provided important information about deformation mechanisms and textures developed under variable thermal regimes and tectonic settings (see e.g. Dietrich and Song, 1984; Schmid et al., 1987; Covey-Crump and Rutter, 1989; Burkhard, 1990; Van Der Pluijm, 1991; Rutter, 1995). Deformation history and evolution of microstructures in large-scale thrust systems depends on the geometry of faults, total fault displacement and on thermal evolution of the thrust zone as well as composition of circulated fluids (Thompson and Ridley, 1987; Knipe, 1990). Underthrusting of continental crust in orogenic zones is associated with a progressive temperature and pressure increase and strong deformation of the underthrust plate (e.g. Štípská and Schulmann, 1995). Subsequent evolution of the thrust array is associated with sequential transfer of displacement into successively lower faults and the building of an imbricated nappe system (Knipe, 1989). The superposition of microstructures that develop during reactivation of previously underthrust rocks by later faulting is common in progressive deformation of nappes at varying PT conditions (Schmid, 1982; Knipe, 1990).

We examined microstructures developed in marbles from a complex imbricated nappe system with well-developed inverted Barrovian metamorphic zonation (Schulmann et al., 1991, 1994). Strongly sheared marbles in units that reached greenschist facies peak metamorphism form major tectonic boundaries, whereas those from units metamorphosed under peak amphibolite facies conditions form boudins surrounded by less competent lithologies. The marbles therefore exhibit different rheological behaviour at different crustal depths during their PTṫ history. In this work we have used published PT calculations from

* Corresponding author. Correspondence address: Laboratoire de Tectonophysique, Université de Montpellier II, 34095 Montpellier, France. Tel.: +33-6714-3602; fax: +33-6714-3603.
E-mail address: stano@dstu.univ-montp2.fr (S. Ulrich).

0191-8141/02/$ - see front matter
PII: S0191-8141(01)00132-8

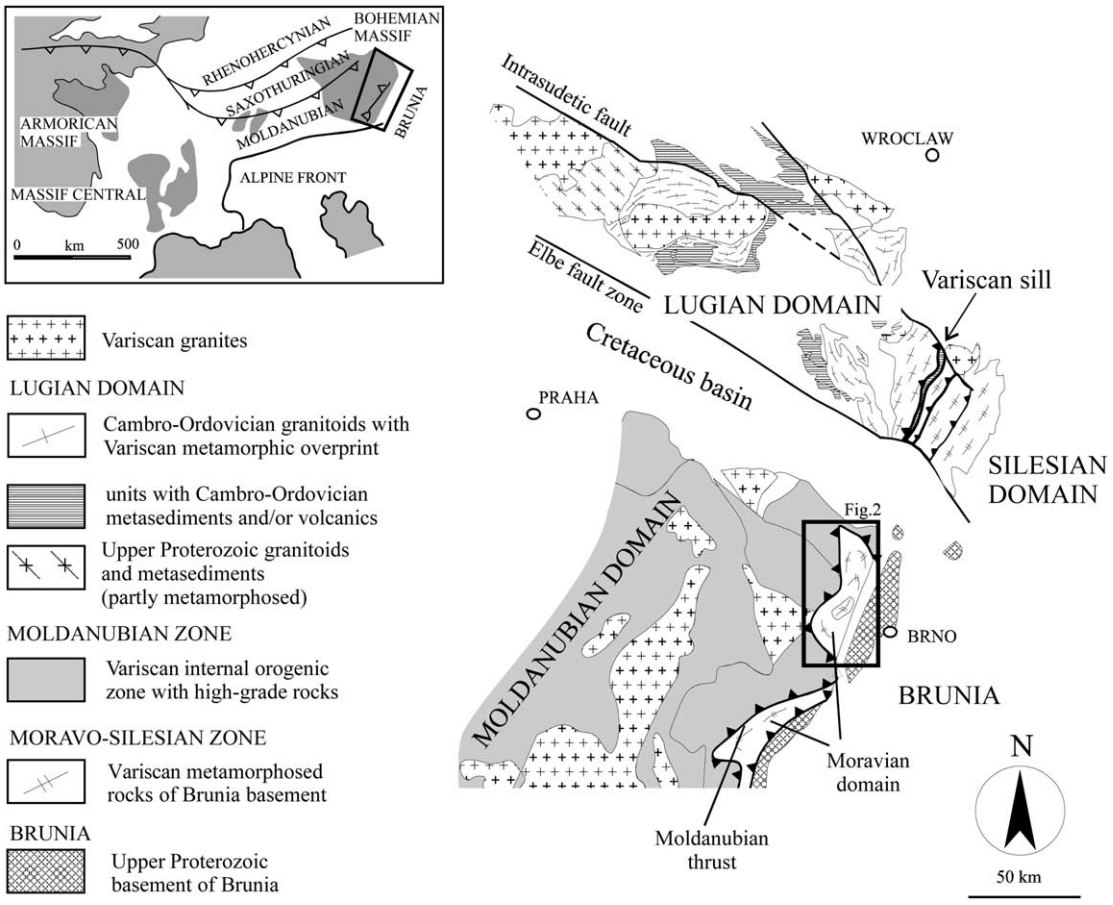

Fig. 1. Sketch map of the Bohemian Massif showing major units of the eastern part of the Massif. The upper left inset shows the position of the studied area within the European Variscides.

metapelites with carbon isotope thermometry and fluid inclusion investigations to estimate peak and retrograde PT conditions in individual units. Detailed microstructural analysis from marbles of all units and metamorphic grades include computer-aided quantitative analysis of grain boundaries, grain shapes and grain sizes, texture goniometry and universal stage study of calcite microfabrics. These data were used to determine deformational mechanisms and flow stress. An attempt was made to attribute microstructures, inferred deformation mechanisms and stress estimates to major deformational episodes.

The aims of this contribution are to provide: (1) a description of microstructural evolution and a definition of deformation mechanisms in marbles during continental underthrusting and prograde metamorphism; (2) identification of deformation microstructures and deformation mechanisms associated with nappe stacking; (3) estimates of flow stress and strain rates of individual deformational and metamorphic episodes; and (4) an explanation of different mechanical responses of marbles from individual metamorphic units to continental underthrusting and subsequent differential strain localisation during nappe stacking.

2. Geological setting

The eastern margin of the Bohemian Massif is built up of Cadomian crust belonging to the Brunia microcontinent (Dudek, 1980) and of high-grade schists, gneisses, migmatites and granulites of the internal Variscan–Moldanubian zone (Suess, 1912). The internal zone was thrust eastwards over Brunia foreland during the Variscan orogeny along the large-scale Modanubian thrust. The western margin of Brunia and its Devonian sedimentary cover was imbricated and metamorphosed to form a belt of Variscan Nappes called the Moravo–Silesian zone. This zone represents a 300-km-long and about a 50-km-wide Variscan collision front emerging through the overthrust Modanubian Nappe of Suess (1926) in the form of two large-scale tectonic windows: the southern Thaya window and the northern Svratka window of Suess (1912, 1926) (Fig. 1).

The Svratka window is built from two crystalline Brunia derived nappes overlying Cadomian basement and its Devonian cover (Fig. 2). The lithotectonic structure is characterised from bottom to top and from East to the West as follows. (1) The Parautochthonous domain (PA) consisting of various types of igneous and metamorphic

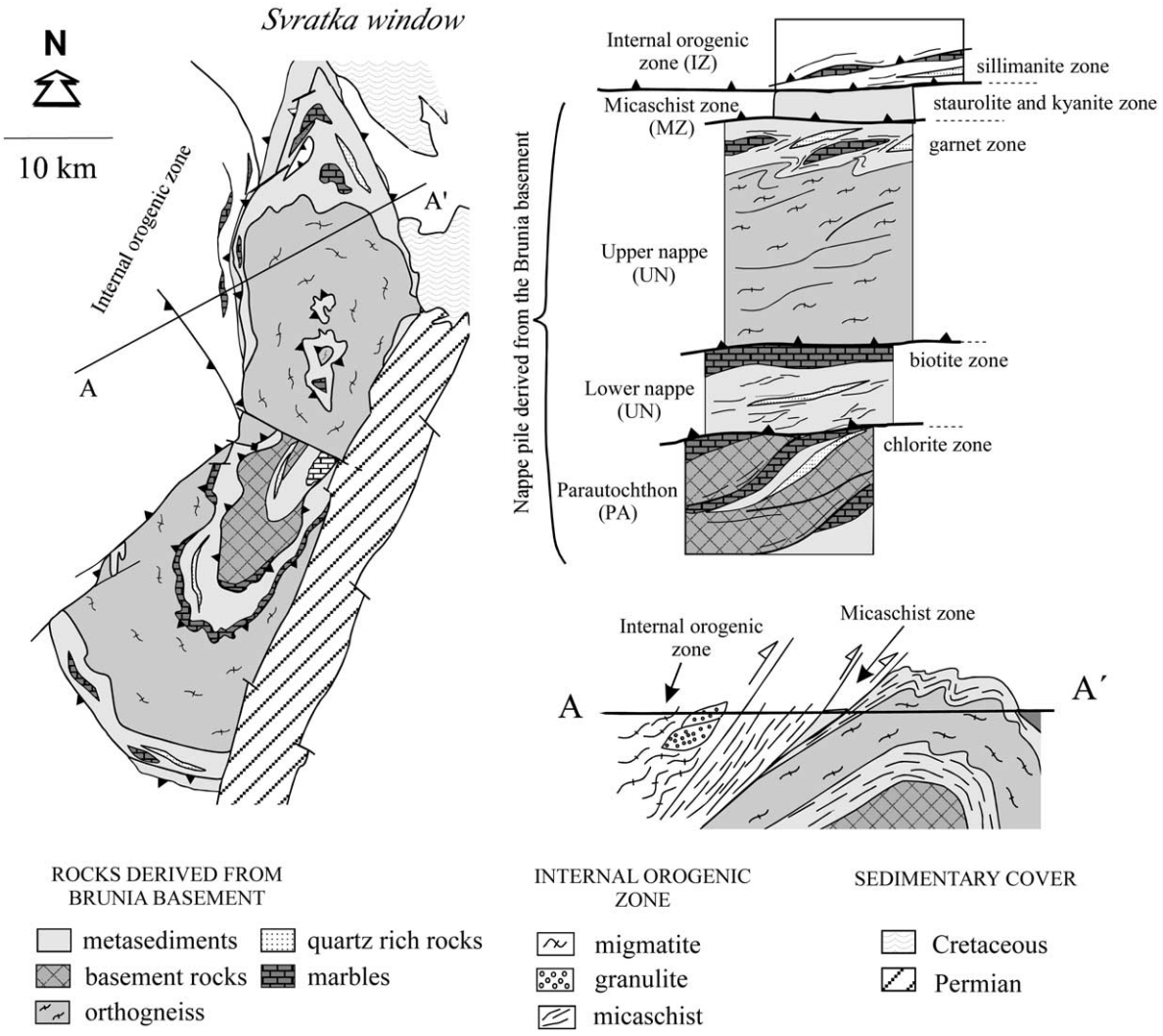

Fig. 2. Synoptic geological map of the Svratka window showing the major nappe structures. The lithotectonic column and cross-section of the northern termination of the Svratka window show relationships between the main tectonic units, lithotectonic boundaries and inverted metamorphic zonation.

rocks of Neo-Proterozoic age (Fritz et al., 1994) unconformably covered by a shallow marine Devonian sedimentary sequence of Pragian to Givetian age, containing marbles, quartzitic metapebbles and schists (Chlupáč, 1994). (2) The Lower Moravian Nappe (Lower Nappe, LN) is composed essentially of biotite micaschists with intercalations of quartzites. A continuous marble layer tens to 100 m thick forms the top of the Nappe. (3) The upper Moravian Nappe (Upper Nappe, UN). The bottom of the nappe consists of a 2–3-km-thick orthogneiss body intercalated with amphibolites in its upper part. The top of the Nappe is formed by garnetiferous micaschists containing numerous boudins of marbles. Quartzites appear in the northern part of the window in the form of thin lenses surrounded by quartz-rich metapelites.

The so-called Moravian micaschist zone (Micaschist Zone, MZ) (Suess, 1926) forms the boundary between the Moravian zone and the Moldanubian zone farther to the west. This unit consists dominantly of a monotonous sequence of staurolite and kyanite micaschists containing boudins of high-grade amphibolites, granulites and eclogites. Farther to the west, occurs a marginal unit of the Variscan internal zone (the Svratka crystalline unit—the Internal Zone, IZ) and consists of garnet–sillimanite micaschists associated with migmatites and orthogneisses. Marble boudins form a girdle at the base of this unit.

2.1. Structural evolution

The first event, D1, is interpreted as being the result of progressive underthrusting of Cadomian continental lithosphere below the internal Variscan zone and is associated with development of prograde Barrovian metamorphism within the underthrust Cadomian basement (Štípská and Schulmann, 1995). During this event, the main metamorphic fabric and a range of ductile structures (e.g. isoclinal synschistose folding and mineral lineations) developed in all units of the Moravo–Silesian zone

(Schulmann et al., 1991, 1994). The underthrusting event is manifested in the field by development of D1 shear zones affecting crystalline basement of the Parautochthon, pervasive deformation of marbles and metaconglomerates and local appearance of early metamorphic fabric in unretrogressed garnetiferous micaschists of the Lower Nappe. In the Upper Nappe and the Internal Zone, the D1 deformation is marked by pervasive development of a medium-grade metamorphic foliation in micaschists, in coarse-grained marbles, and in orthogneiss.

The second major event, D2, is connected with imbrication of previously underthrust Cadomian basement and the development of two large-scale crystalline Nappes responsible for the inversion of Barrovian metamorphic zonation (Štípská and Schulmann, 1995). During this event, the lowermost Parautochthon unit was affected by thin-skinned tectonics forming the basement and cover hinterland dipping duplexes associated with strong recrystallisation of marbles along high strain zones. In the Lower Nappe, the D2 deformation is dominant leading to the almost complete mylonitic reworking of marbles. In the Upper Nappe high strain D2 shear zones affect mainly the orthogneiss body at the bottom of this unit and locally metasediments higher in the sequence.

The D3 event is observed only in the upper part of the nappe pile where all previously formed fabrics are affected by localised extensional shear zones, which result from synconvergence collapse of the nappe pile in the late stages of thrusting (Schulmann et al., 1994). Foliation within these shear zones is associated with greenschist facies retrogression in metapelites and with strong grain-size reduction in marbles.

2.2. Metamorphic evolution

The metamorphic pattern of the Svratka window is characterised by well-developed Barrovian metamorphic inverted zonation (M_1) ranging from chlorite to sillimanite zone (Schulmann et al., 1991) (Figs. 2 and 3). Peak PT conditions throughout the whole Nappe pile were estimated using metapelite thermobarometry. From the bottom to the top of the Nappe pile the metamorphic zonation is defined

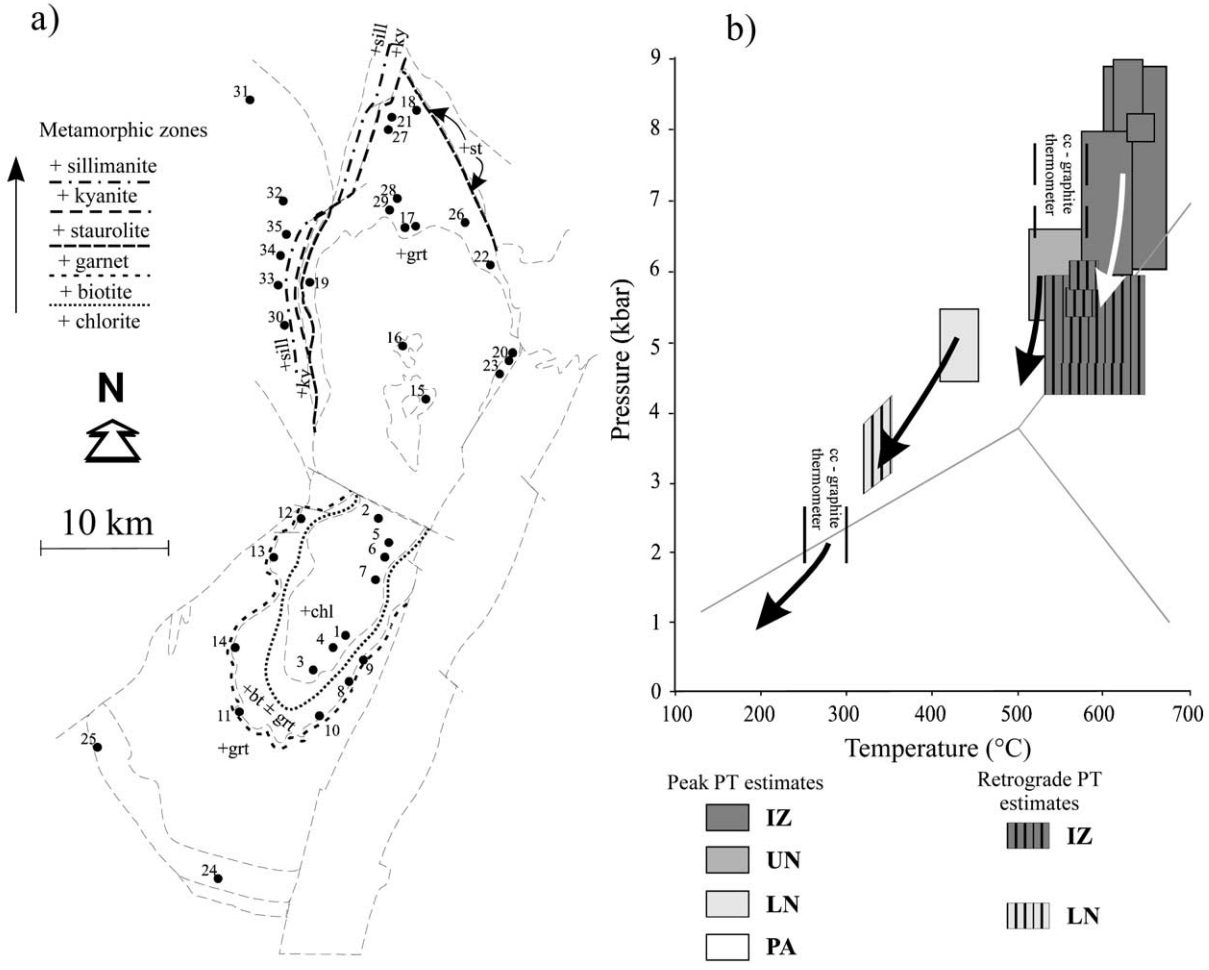

Fig. 3. (a) Outlines of the main tectonic units in the area studied and the sampling sites for the marbles used in this study coupled with metamorphic isograds. The site numbers correspond to those given in Table 1. (b) A P–T diagram shows results of previously published geo-thermobarometric data from the studied area.

Table 1
A list of the values that results from the quantitative microstructural analysis for each sample and microstructural type

Unit	Number of specimens		$\Delta A(\alpha)$	$\Delta\alpha$	Av. D (μm)	Note
PA	1	U42	0.21	74	133	Type 1
	2	U7	0.2	76	165	Type 1
	3	U18	0.18	73	185	Type 1
	4	U17	0.31	72	33	Type 2
	5	U49	0.25	70	39	Type 2
	6	U53	0.33	72	57	Type 2
	7a	U72	0.22	65	29	Type 2
	7b	U72sup	0.2	70	14	Type 2
LN	8	N88	0.36	80	425	Type 2
	9a	N91	0.39	74	278	Type 2
	9b	N91	0.3	83	794	Type 1
	10	N92	0.28	77	332	Type 2
	11	U120	0.48	76	354	Type 2
	12	U36	0.48	78	404	Type 2
	13	U39	0.46	82	425	Type 2
	14	U66	0.46	78	326	Type 2
UN	15	U30	0.41	76	342	Type 2
	16	U33	0.44	83	334	Type 2
	17a	U12	0.27	73	740	Type 1
	17b	U12	0.32	77	351	Type 2
	18	U62	0.16	67	968	Type 1
	19	U25	0.18	61	566	Type 1
	20a	U32	0.29	75	577	Type 1
	20b	U32	0.36	77	153	Type 3
	21	U60	0.31	74	579	Type 1
	22	U54	0.38	74	186	Type 3
	23	U31	0.39	81	465	Type 2
	24	N79	0.23	70	301	Type 2
	25	N85	0.29	72	282	Type 2
	26	U56	0.24	78	336	Type 2
	27	U74	0.22	61	439	Type 2
	28	U57	0.26	70	375	Type 2
	29	U59	0.26	77	388	Type 2
IZ	30	U46	0.23	61	703	Type 1
	31	U47	0.14	65	1029	Type 1
	32	N71	0.17	72	1526	Type 1
	33	U28	0.28	68	201	Type 3
	34	N102	0.25	72	29	Type 3
	35	N107	0.13	75	64	Type 3

by: (1) the chlorite zone in the Parautochthon has assemblage Chl + Mu in quartzitic Devonian meta-sediments. The temperature of metamorphism was estimated using calcite–graphite thermometry indicating lower greenschist facies conditions that did not exceed 300 °C (Ulrich, 2000). (2) The biotite zone in the Lower Nappe metapelites characterised by the assemblage Mu + Chl + Bt ± Mn rich Grt indicating a local transition from biotite to garnet zone ($T = 430$–450 °C at $P = 4.5$–6 kbar; Weber, 1996). In order to establish retrograde conditions of metamorphism in this unit a fluid inclusion study was carried out on quartz veins that crosscut the main foliation (Ulrich, 2000). Minimum PT conditions of trapping of H_2O-liquid CO_2 inclusions were estimated at 320–350 °C and 3–4 kbar. (3) The garnet zone developed in metapelites of the lower part of the Upper Nappe is marked by a mineral assemblage Grt + Bt + Mu ± Chl ($T = 500$–560 °C and $P = 5$–7 kbar; Tichý, 1992). The calcite–graphite thermometry from coarse-grained marbles yields a temperature range between 500 and 570 °C (Čížek, 1985). (4) The kyanite zone in metapelites of the MZ show assemblage Ky + St + Grt + Bt + Mu ($T = 580$–620 °C at $P = 6$–8 kbar; Johan et al., 1990; Tichý, 1992). (5) The sillimanite zone developed in the Internal Zone shows the mineral assemblage Sill ± Ky + Grt + Bt + Mu. The relict peak assemblage Ky + St + Bt preserved in the form of inclusions in garnet porphyroblast was used to estimate temperatures of 610–640 °C at 8–9 kbar (Pitra and Guiraud, 1996). The retrograde stage M2 in this unit is marked by growth of sillimanite at the expense of garnet and kyanite at conditions of 570–640 °C at 4–6 kbar (Pitra and Guiraud, 1996; Štoudová, 1998).

3. Microstructures

The microstructural characteristics of grain size, grain shape, orientation distribution of long axes of grains, shapes of grain boundaries and their configuration with respect to foliation were systematically studied in marbles throughout the whole Nappe pile and in relation to metamorphic grade. Calcite marbles from 35 localities are presented in this work (Fig. 3).

3.1. Techniques

Thin sections were cut perpendicular to the macroscopically determined foliation and parallel to the lineation (*XZ* section of finite strain). In the case of fine-grained samples, *XZ* surfaces were polished and subsequently etched by acetic acid (2% solution for 120 s). Grain boundaries of at least 150 grains from each sample were traced using an optical microscope for coarse-grained samples and using a CamScan scanning electron microscope for fine-grained aggregates and then digitised.

A quantitative microstructural analysis of grain boundaries was carried out on such images using surface analysis and volume analysis projection methods (Panozzo, 1984). The surface analysis was used to determine the grain boundary orientation distribution, whereas volume analysis was applied to the orientation distribution of long axes of grains. Therefore, the typical data set of each unit and for both coarse-grained and fine-grained microstructure includes an orientation distribution function and rose diagram of the grain boundaries together with a rose diagram of long axes of grain orientation distribution. The results are expressed using $A(\alpha)$ values, which represent normalised intensity of grain boundary orientation. The $\Delta A(\alpha)$ represents the difference between the maximum and the minimum of the orientation function and characterises the intensity of grain boundary orientation alignment. The angular difference $\Delta\alpha$ between the minimum and maximum

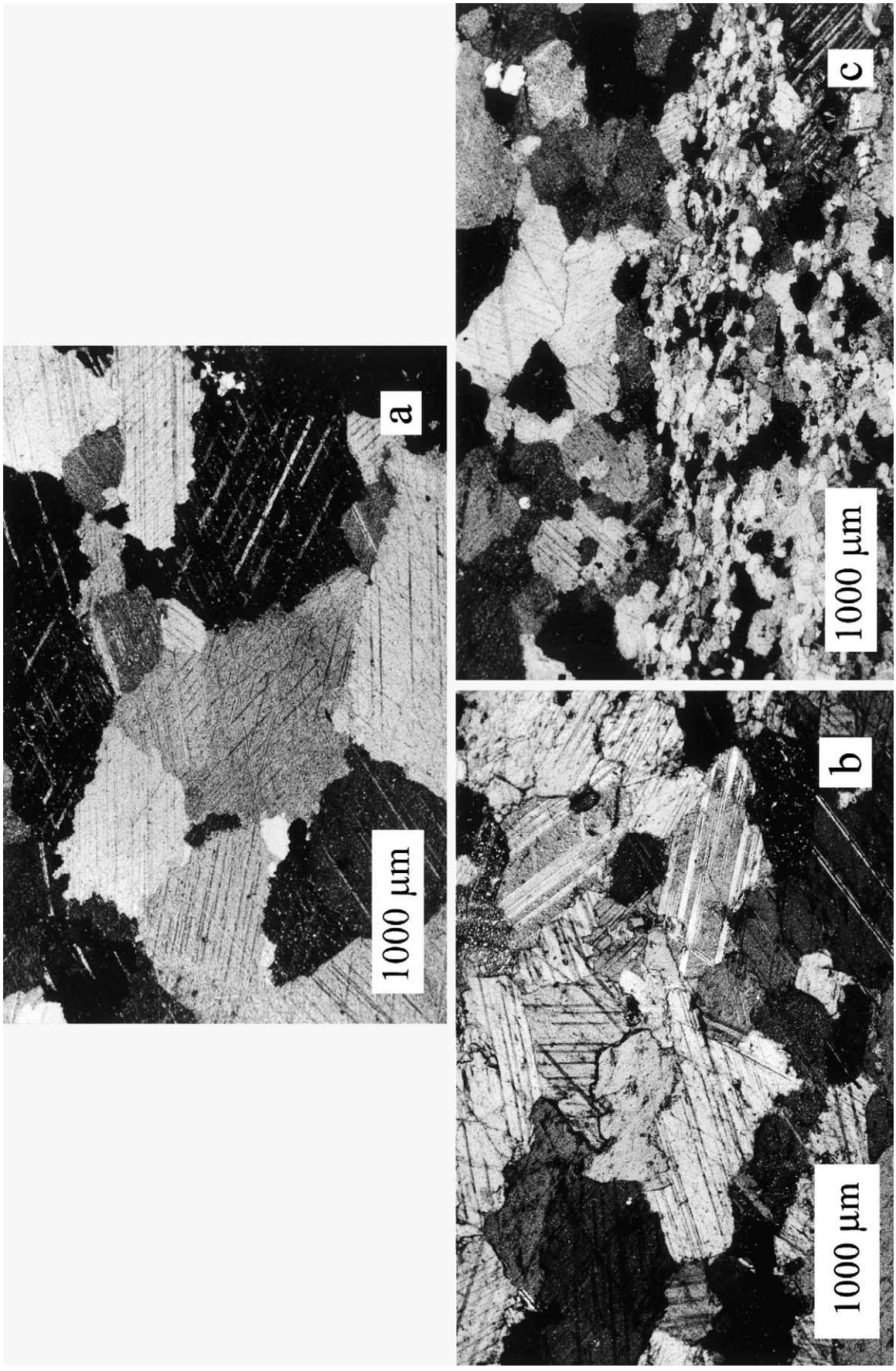

Fig. 4.

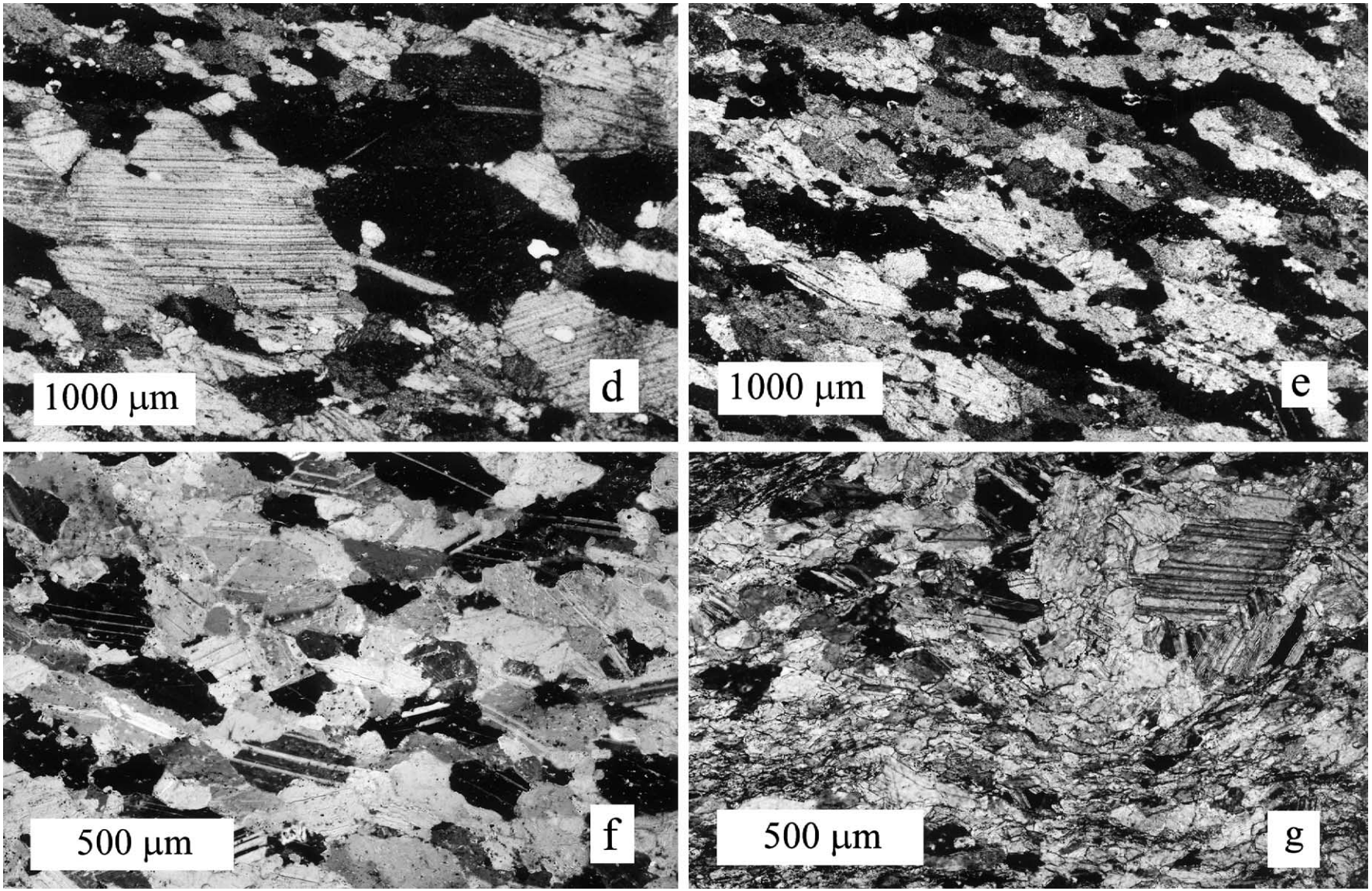

Fig. 4. (*continued*)

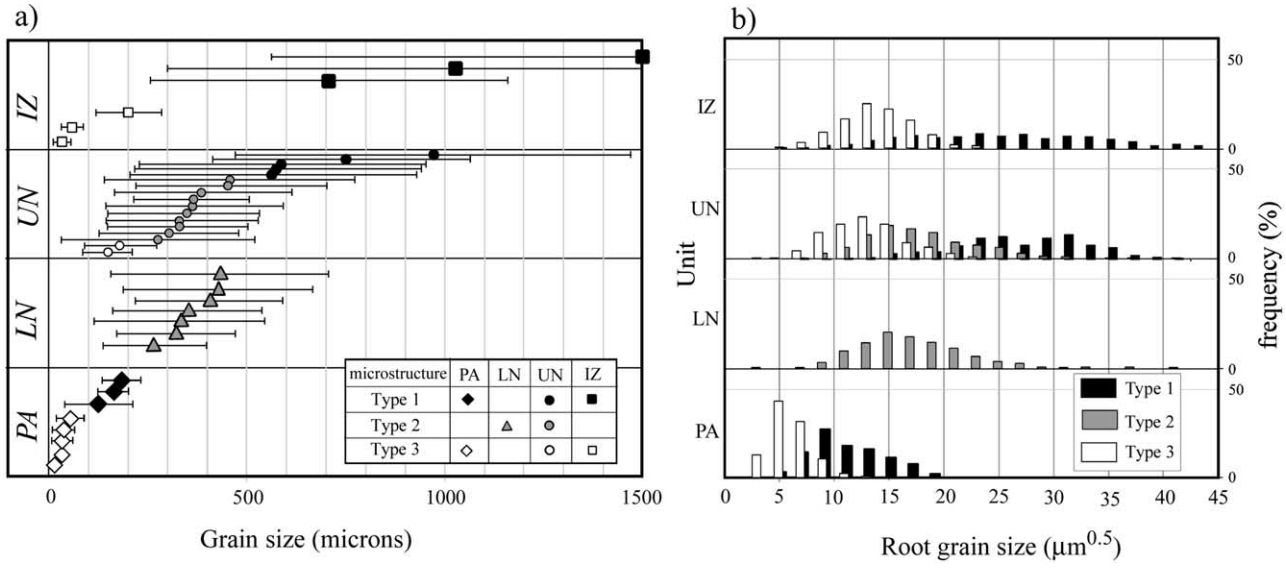

Fig. 5. Results of grain-size analysis from all units and microstructural types are represented by different symbols, as indicated. (a) Calculated average grain size and standard deviation. (b) Histogram showing the most typical frequency distribution of grain size according to the type of microstructure.

length projection defines symmetry characteristics. A value of $\Delta\alpha = 85–90°$ corresponds to a grain boundary configuration that is symmetric with respect to foliation trace, whereas $\Delta\alpha < 85°$ indicates asymmetrical bimodal distribution.

Grain-size analysis was carried out together with quantitative numerical microstructural analysis using digitised images. The calculated Feret diameter D of all grains has been corrected because of truncation effect using the expression $\delta = (4/\pi) \times D$ (Exner, 1972), where δ is a real grain diameter. Measured data were presented in diagrams expressing average grain size, standard deviation and characteristic frequency histograms of grain size distribution. Resulting values of quantitative microstructural analysis and grain size analysis are presented in Table 1.

3.2. Results of microstructural analysis

Three main types of microstructure were recognised in the Nappe pile according to grain size, grain shape characteristics and relationships with respect to macroscopic structures. Type 1 is a coarse- to medium-grained microstructure with sub-equant grain shapes developed in the main metamorphic foliation S1 and synschistose isoclinal folds F1 in all tectonic units. Type 2 is a medium-grained microstructure with elongate grain shapes mainly developed in the highly strained D2 zone in the footwall of the Upper Nappe and along more localised D2 shear zones affecting marbles in the Upper Nappe. Type 3 is a mylonitic fine-grained microstructure with elongate or sub-equant shapes developed in thrust related D2 shear zones reworking D1 fabrics of the Parautochthon and in localised extensional D3 shear zones affecting previous fabrics of the Upper Nappe and the Internal Zone.

3.2.1. Type 1 microstructure

A coarse-grained fabric in marbles of the Parautochthon is locally preserved despite intense late reworking. Slightly elongate grains, 130 microns in average size, show straight to irregular grain boundaries with weak shape preferred orientation (Fig. 4f). Common thick twins with regular, as well as irregular shapes, correspond to twin Type III of Burkhard (1993). Rare relics of Type 1 microstructure in the Lower Nappe include polycrystalline aggregates (Fig. 4d) of lenslike shape surrounded by a medium-grained recrystallised groundmass. These aggregates consist of elongate large grains with weakly lobate boundaries. In the Upper Nappe, Type 1 microstructure is common, being marked by large subequant to slightly elongate grains with strongly migrated boundaries (Fig. 4b). The intensity of grain-shape preferred orientation varies from weak to strong alignment in individual samples. In the Internal Zone, large subequant grains dominate with lobate to straight grain boundaries. In the Upper Nappe and the Internal Zone, calcite grains exhibit thick, patchy shaped

Fig. 4. Photomicrographs showing characteristic microstructures of marbles: (a) and (b) Type 1 microstructure from the Internal Zone and the Upper Nappe, respectively. Coarse calcite grains show migrated grain boundaries. (c) Type 3 microstructure from the Upper Nappe developed along heterogeneous shear zone. (d) Relict coarse calcite grains of the Type 1 microstructure from the Lower Nappe. (e) Characteristic elongate grains of the Type 2 microstructure from the Lower Nappe. (f) Coarser grain microstructure Type 1 from the Parautochthon unit that is preserved in the low strain domains. (g) Mylonitic Type 2 microstructure from the Parautochthon shows intense grain size reduction.

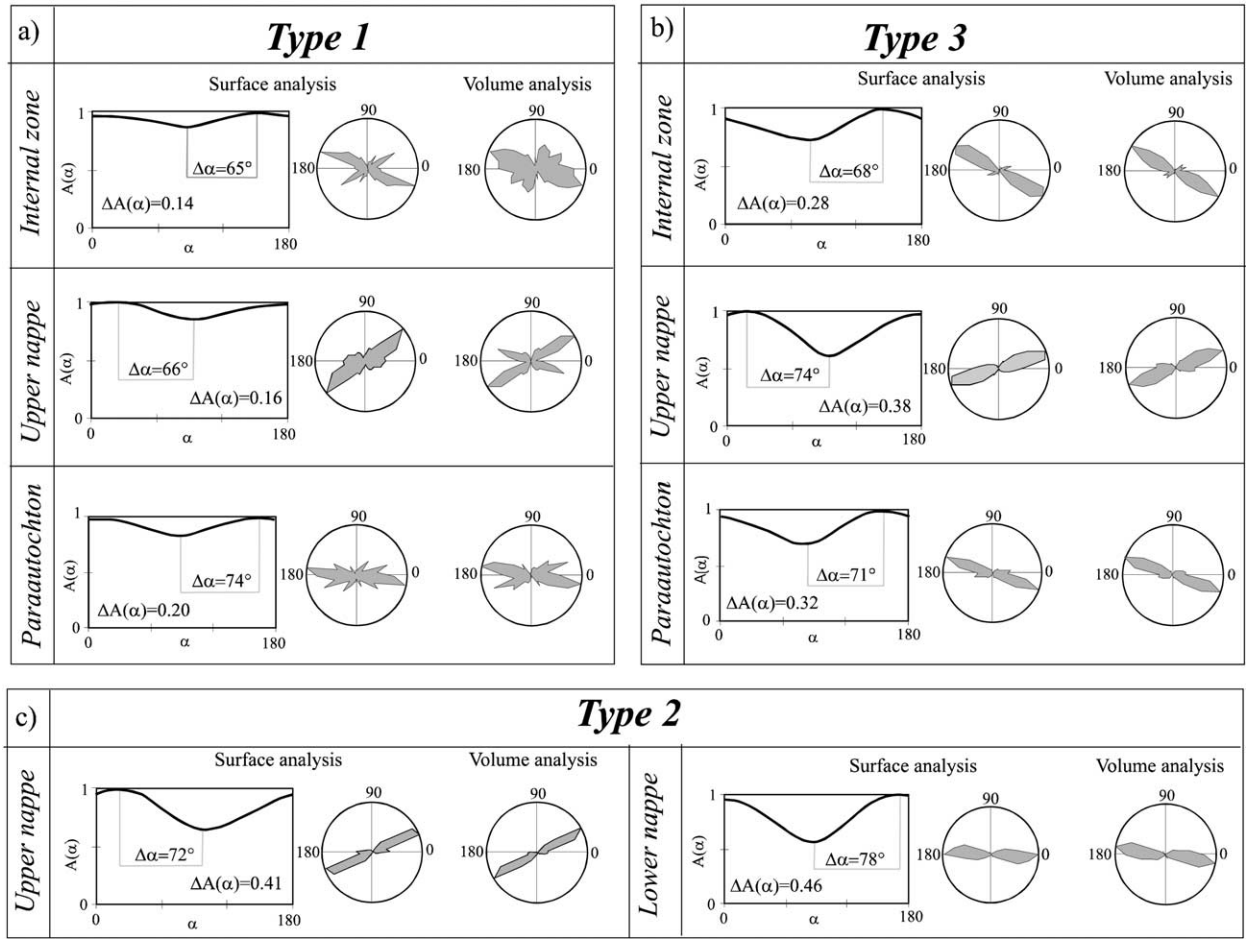

Fig. 6. Results of surface and volume analysis projection methods for all types of microstructures and units represented by normalised intensity of grain boundary orientation $A(\alpha)$-α diagrams of Panozzo (1984), and rose diagrams of grain boundaries and rose diagrams of long axes of grain orientation distribution. The angular difference $\Delta\alpha$ between minimum and maximum length projection defines the degree of symmetry of grain shapes.

twins of type IV of Burkhard (1993) with sutured twin boundaries. The grain sizes in the Upper Nappe range from 340 to 740 microns and in the Internal Zone vary between 700 and 1500 microns (Fig. 5a).

Grain-size frequency histograms for Type 1 microstructure of the Parautochthon show a strong unimodal maximum and are skewed towards large grain size (Fig. 5b). Frequency histograms for the same microstructure in the Upper Nappe and the Internal Zone display nearly symmetrical and weakly bimodal distribution. Type 1 microstructures are marked by weak orientation distribution of grain boundaries ($\Delta A(\alpha) = 0.1$–0.3) and weak shape preferred orientation identified by volume analysis (Figs. 6a and 7). Values of $\Delta\alpha$ (65–80°) indicate strong asymmetry of grain boundary surfaces with respect to grain alignment in the whole Nappe pile (Fig. 7).

3.2.2. Type 2 microstructure

The Type 2 microstructure is dominant in the Lower Nappe and reworks almost totally the Type 1 fabric. New grains are characterised by strongly elongate shapes with irregular boundaries and grain size in the range of 300 to 430 microns (Fig. 4e). Differences in shape and size of calcite grains result from the local presence of micas. Pure marbles show strong grain shape preferred orientation with the long axes at an angle of 40° with respect to mesoscopic foliation. The impure marbles show also grain shape preferred orientation but parallel to micas defining the main planar fabric. In the Upper Nappe, Type 2 microstructure is common and is characterised by significant grain elongation, serrate grain boundaries and grain size varying between 280 and 460 microns. Frequency histograms show unimodal distribution skewed to larger grains (Fig. 5). The diagrams in Fig. 6 indicate a strong intensity of grain boundary preferred orientation ($\Delta A(\alpha) = 0.3$–0.5) for Type 2 microstructure in both Lower Nappe and Upper Nappe. Values of $\Delta\alpha$ range between 75 and 82° for both Lower Nappe and Upper Nappe marbles (Figs. 6c and 7).

3.2.3. Type 3 microstructure

Type 3 microstructure associated with D2 shear zones is

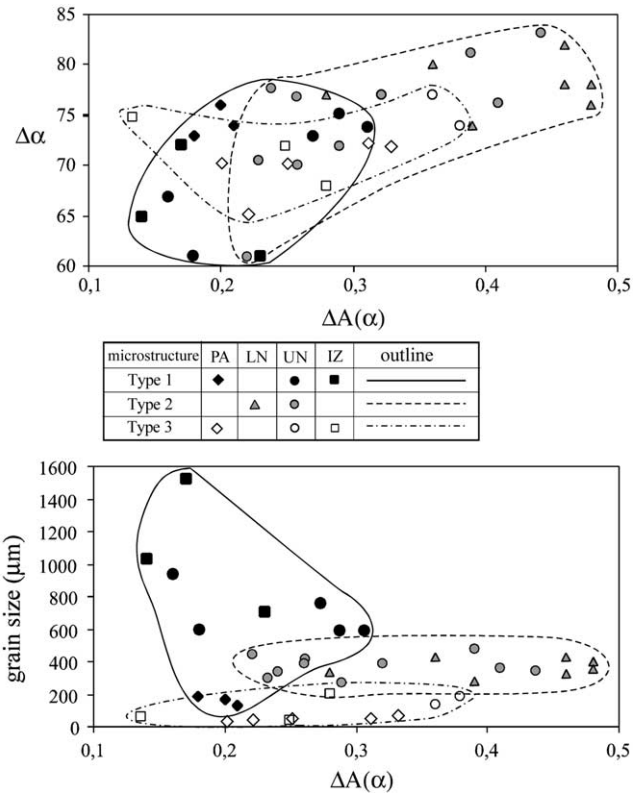

Fig. 7. Diagrams show relationships between intensity $\Delta A(\alpha)$ and symmetry $\Delta\alpha$ of grain boundary orientation distribution and grain size resulting from the quantitative microstructural analysis. Microstructural Types 1, 2 and 3 are distinguished.

dominant in the Parautochthon and results in significant modification of the early Type 1 coarse-grained fabric. Recrystallised small grains (Fig. 4g) typical of transitional core and mantle microstructure envelope the relics of Type 1 grains (White, 1976). A fully recrystallised Type 3 microstructure is characterised by grain size ranging from 14 to 57 microns. This recrystallised matrix is often concentrated into high strain zones surrounding lenses with preserved coarse-grained microstructure. The degree of grain elongation slightly decreases with decreasing grain size. The intensity of grain boundary preferred orientation is $\Delta A(\alpha) = 0.2–0.35$ and the symmetry of grain boundary configuration is $\Delta\alpha = 65–72°$ (Figs. 6b and 7).

This microstructure is also developed in the Upper Nappe and Internal Zone along localised D3 extensional shear zones crosscutting the coarser-grained Type 1 fabric. Here, the deformation is connected with intense grain-size reduction via the sub-grain rotation recrystallisation mechanism (Fig. 4c). New grains are strongly elongate, with straight grain boundaries and an average grain size of 180 microns. The frequency histograms of grain size show symmetrical distribution (Fig. 5). The grain boundary preferred orientation is strong ($\Delta A(\alpha) = 0.28–0.38$) and configuration of grain boundaries with respect to foliation is asymmetrical ($\Delta\alpha = 68–77°$) (Figs. 6 and 7).

3.3. Summary of quantitative microstructural analysis

Quantitative microstructural analysis shows that the intensity of grain boundary preferred orientation $\Delta A(\alpha)$ increases in conjunction with the increasing degree of grain boundary symmetry $\Delta\alpha$ in the case of microstructures of Type 2 and 3. In contrast, the microstructure of Type 1 shows only small variations in both $\Delta A(\alpha)$ and $\Delta\alpha$ values (Fig. 7a). Fig. 7b shows that the intensity of grain boundary preferred orientation $\Delta A(\alpha)$ decreases with increasing grain size for Type 1 microstructure. There are no systematic relationships between the intensity of grain boundary preferred orientation and grain size for Type 2 and 3 microstructures. However, the intensity of grain boundary preferred orientation $\Delta A(\alpha)$ increases in conjunction with the increasing grain size when comparing Type 2 and 3 microstructures (Fig. 7b).

4. Textures

X-ray textures of calcite were determined using a Scintag XDS 2000, computer-controlled texture goniometer with a solid-state detector in ETH Zurich using the combined reflection- and transmission, scan method, Ca-Kα-radiation, and a counting time 1.5 s per 5° step. Diffraction peaks 001(c), 110(a), 018(e) 012(f), 104(r), 113, and 202(h) were measured. The pole figure scans were combined to give inverse pole figures using the harmonic method as described by Casey (1981). Samples with large grain size were measured using a universal stage mounted on an optical microscope. The specimens were cut parallel to the mineral and stretching lineation and perpendicular to foliation. Texture (lattice preferred orientation—LPO) of characteristic specimens is presented by an inverse pole figure calculated for the foliation plane normal, calculated *c*-axes pole figures and *a*-planes and *e*-planes pole figures. The results of universal stage measurements are presented using *c*-axis pole figures.

Type 1 microstructure from the Parautochthon is characterised by a weak crystallographic preferred orientation in all samples marked by a single maximum of *c*-axes normal to the foliation and a weak maximum in the inverse pole figure. Pole figures for *a*-planes are oriented along the great circle parallel of the foliation plane, and *e*-planes exhibit a single maximum perpendicular to the foliation plane (Fig. 8). Type 1 microstructure in the Upper Nappe shows one maximum parallel to the elongation direction of calcite crystals, and the second close to the mesoscopic foliation corresponding to maxima 2 and 3, respectively, of Schmid et al. (1987). These maxima are interpreted as resulting from activity of r- and f-slip systems. Lack of the third maximum perpendicular to the foliation (maximum 1), known from experimental works (Kern and Wenk, 1983; Schmid et al., 1987) suggests absence of basal *a*-slip. *C*-axis pole figures of Type 1 microstructure from the Internal Zone show a

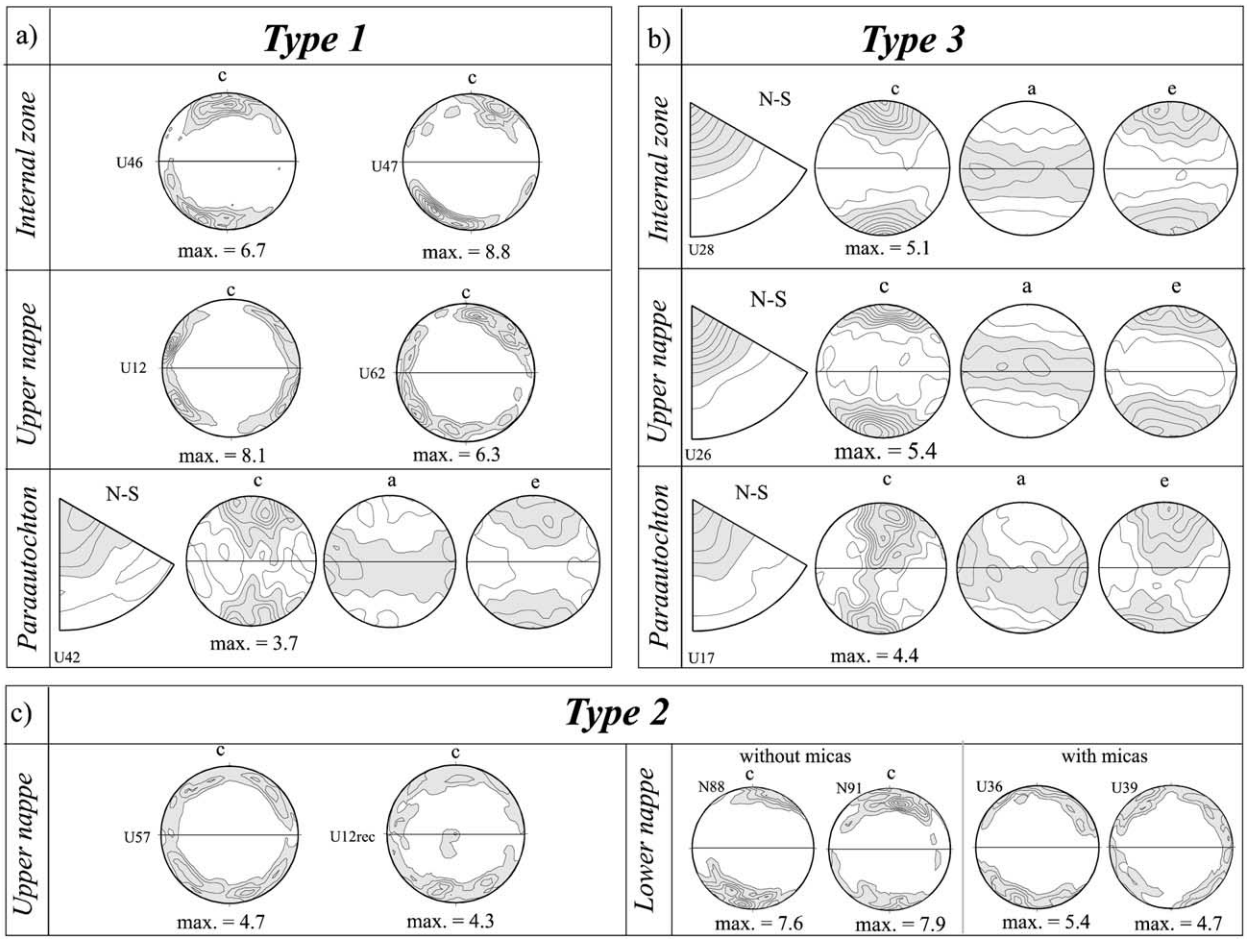

Fig. 8. Results of textural analysis for all types of microstructures and corresponding units. The characteristic sample measured on the texture goniometer is presented as the inverse pole figure calculated for the foliation normal and pole figures of distribution of *c*-axes, *a*-planes and *e*-planes contoured at intervals of 0.5 of a uniform distribution. The results of universal stage measurements are presented using *c*-axis pole figures contoured at intervals of 1.0 of a uniform distribution. The equator and E–W direction in the pole figure correspond to the foliation plane and the stretching lineation, respectively.

strong maximum oriented perpendicular to weak grain shape preferred orientation corresponding to maximum 1 of Schmid et al. (1987).

Type 2 microstructures in the Parautochthon exhibit a weak fabric similar to Type 1 microstructure from the same unit. *C*-axes are oriented along a single girdle slightly oblique with respect to foliation normal and a maximum close to the *Z*-axis of finite strain and *a*-planes form a broad girdle slightly oblique with grain shape foliation. *E*-planes exhibit a single broad maximum perpendicular to foliation. LPO of marbles from the Lower Nappe was determined using the universal stage, and shows two types of fabric. Samples rich in micas are represented by *c*-axis pole figures with two maxima located along the margin of the diagram that correspond to types 1 and 2 maxima of Schmid et al. (1987). Poles to *e*-planes are located along the periphery of the pole figure with a broad maximum perpendicular to foliation. The pole figures of samples without micas show a single peak maximum of *c*-axes normal to the foliation and *e*-planes exhibit a similar pattern to the *c*-axes fabric. Marbles with Type 2 microstructure in the Upper Nappe show two scattered maxima at the periphery of the *c*-axes pole figure. Scattering of the *c*-axes distribution can indicate the beginning of reorientation of the texture into a single maximum type oriented normal to foliation (Casey et al., 1998) (Fig. 8).

The microstructure Type 3 shows moderate to strong fabrics with a single *c*-axis maximum close to the foliation normal. *a*-Planes form a girdle sub-parallel to the foliation and *e*-planes form a single broad maximum close to the foliation pole (Fig. 8).

5. Definition of deformation mechanisms

A deformation mechanism is a microphysical model of how mineral aggregates deform. It carries consequences for the evolution of microstructure and LPO, and for the form of the flow-law. A deformation regime is a region on an experimentally defined deformation regime map in which an empirically fitted flow-law holds. It indirectly suggests a deformation mechanism, but is not synonymous with it.

Schmid et al. (1987) carried out ideal simple shear experiments on Solenhofen and Carrara marbles and results of each run were compared with deformation regimes. Additionally, microstructure and texture analyses were made on these samples in order to establish the main microfabric regimes.

Naturally deformed marbles can be neither plotted into a deformation regimes map nor directly compared with microfabric regimes of Schmid et al. (1987). However, described microstructure and texture of each studied sample can be compared with the results of Schmid et al. (1987) and Walker et al. (1990) and used, together with grain size, in order to estimate the active deformation mechanism.

5.1. Interpretation of Type 1 microstructures and textures

Type 1 microstructure in the Parautochthon, Upper Nappe and Internal zone shows high asymmetry of grain boundary distribution with respect to the direction of grain alignment (lozenge shaped grains) and lobate shape of grain boundaries indicating the grain boundary migration recrystallisation mechanism. In addition, a small value of $\Delta\alpha$ indicates a strong shear component of deformation. Results of surface analysis carried out by Schmid et al. (1987) on samples CT2, CT4 and CT7 deformed in grain boundary migration regime show a higher degree of symmetry ($\Delta\alpha = 73–84°$) and higher intensity of grain boundaries orientation alignment ($\Delta A(\alpha) = 0.31–0.45$) than our samples.

In addition, the textures measured in the Parautochthon and the Upper Nappe are not consistent with texture reported by Schmid et al. (1987) for samples deformed in the grain boundary migration recrystallisation regime. The texture from Parautochthon is marked by weak intensity, whereas texture from the Upper Nappe show maxima that resemble that reported by Schmid et al. (1987) in e.g. sample CT6 deformed in the intracrystalline slip deformation regime. Marbles from the Internal Zone (sillimanite zone) show textures similar to those experimentally developed in twinning, but also in grain boundary migration regime (Fig. 10a and c; Fig. 15f of Schmid et al., 1987).

We suggest that the grain boundary migration recrystallisation was the dominant process responsible for shapes of grain boundaries and was associated with grain growth. The texture may well have formed later at lower temperatures (Schmid et al., 1987). In conclusion, despite discrepancies between naturally and experimentally developed textures, we suggest that the mechanism of dislocation creep and grain boundary migration recrystallisation was the dominant process during development of Type 1 microstructure.

5.2. Interpretation of Type 2 microstructures and textures

The strong flattening of grains, increase in grain boundary symmetry ($\Delta\alpha$) and elongation of grains characterise the Type 2 microstructure. Results of quantitative microstructural analysis are consistent with those of Schmid et al. (1987) developed in the intracrystalline slip regime. An important feature in marbles with the Type 2 microstructure is a decrease in grain size with respect to Type 1 microstructure. These characteristics with moderate *c*-axis preferred orientation could be interpreted as resulting from a mechanism of dislocation creep together with subgrain rotation recrystallisation. However, serrate grain boundaries may imply the influence of grain boundary migration mechanism on newly formed grain boundaries. Schmid et al. (1987) and Walker et al. (1990) observed similar microstructures in the intracrystalline slip regime and high stress grain-size sensitive regime, respectively. However, our *c*-axis pole figures are consistent with those related to the regime of the experimental work of Walker et al. (1990). Therefore we suggest that the main deformation mechanism is the dislocation creep with possible (and subordinate) contribution of grain boundary sliding.

5.3. Interpretation of Type 3 microstructures and textures

The characteristic feature of Type 3 microstructure is the core–mantle structure and the development of a recrystallised fine-grained groundmass. Recrystallisation occurs via sub-grain rotation leading to the formation of sub-equant to elongate fine grains. These microstructural observations together with weak textures may be compared with the microstructure and textures of the high stress, grain size sensitive regime for elongate grains and that of the low stress, grain size sensitive regime for sub-equant grains (Walker et al., 1990). We suggest that this microstructure and constantly weak texture result from partitioning of deformation on the grain scale into intra-crystalline and inter-crystalline deformation mechanisms (Casey et al., 1998). Therefore the contribution of diffusion creep seems to be dominant during development of the Type 3 microstructure.

6. Paleopiezometry

Several approaches and models were proposed to determine a flow stress at the time of deformation termed paleopiezometry. Existing models are based on, among other things, unbound dislocations density (Kohlstedt and Weathers, 1980); subgrain and dynamically recrystallised grain size (e.g. Mercier et al., 1977; Poirier, 1985); or a glide-induced deformation lamellae model (Ave Lallemand and Carter, 1971). The dynamically recrystallised grain-size paleopiezometer is widely used by geologists working in the field because of its simple applicability. Unlike paleopiezometers based on dislocation density and subgrain diameter, there is currently no theory to account for the empirical relationship between stress and dynamically recrystallised grain size.

An experimentally defined empirical relationship

between grain size and flow stress is defined as:

$$\Delta\sigma = A \times D^{-n} \quad (1)$$

where $\Delta\sigma$ is the flow stress expressed in MPa, D is the grain diameter expressed in microns, and A and n are dimensionless empirically determined material constants. This simple equation is widely used in studies of naturally deformed rocks. However, grain-size paleopiezometers can only be applied to dynamically recrystallised grains that have not undergone static grain growth and which do not contain second phase particles. This paleopiezometer is valid only if the mechanism of dynamic recrystallisation is the same in nature as that derived from experimental works.

The grain size of all samples and types of microstructures were plotted on a log grain size versus log stress diagram. The type of recrystallisation mechanisms was used for the selection of the appropriate paleopiezometric equation. Therefore, the grain boundary migration paleopiezometer of Rutter (1995) was used for Type 1 microstructure. The flow stress of marbles with the Type 2 microstructure was calculated using both grain boundary migration and sub-grain rotation paleopiezometers after Rutter (1995) and Schmid et al. (1980) following the microstructural arguments mentioned above.

Type 1 microstructures exhibit a systematic decrease in flow stress with metamorphic grade from 50 MPa in the lowest grade (Parautochthon) to around 5 MPa in the highest grades (Internal Zone). Providing that the grain boundary migration recrystallisation mechanisms are accepted for Type 2 microstructure in the Lower Nappe and Upper Nappe, then the flow stress for both units range between 10 and 20 MPa (Fig. 9). If the Type 2 microstructure in these units originated through the dominant contribution of sub-grain rotation recrystallisation, then the flow stress would have values of 2–6 MPa indicating a decrease in stress level with respect to Type 1 microstructure.

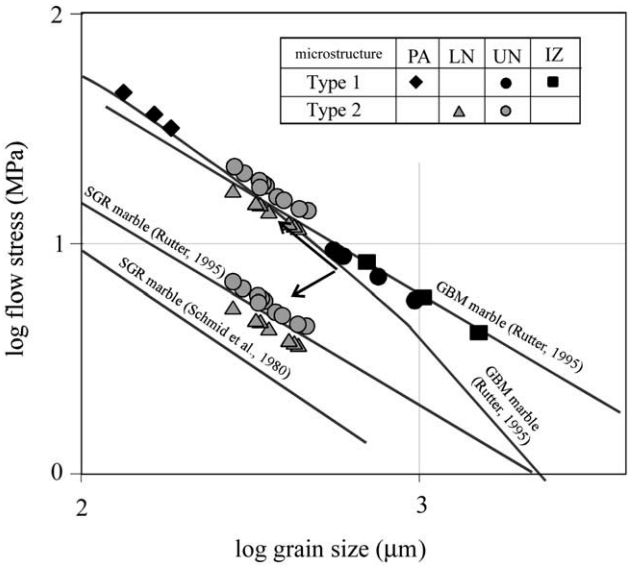

Fig. 9. Log differential stress versus log grain size diagram showing flow stress estimates for each sample marked by symbols indicating the unit and type of microstructure. Grain boundary migration (GBM) paleopiezometer of Rutter (1995) was used for the Type 1 microstructure and for the Type 2 microstructures in the LN and UN. Sub-grain rotation (SGR) paleopiezometers after Rutter (1995) and Schmid et al. (1980) were applied for the Type 2 microstructure in the UN and LN. Arrows indicate possible stress evolutions. See text for explanation.

7. Discussion

7.1. Correlation of microstructural types with tectonic events

An attempt is made to correlate the microstructural Types 1, 2 and 3 with major events in continuous evolution of continental underthrusting and Nappe stacking.

The tectonic model of the studied area suggests a continental underthrusting of Proterozoic basement and its Devonian cover below an orogenic internal zone to the West (Schulmann et al., 1991). PT estimates obtained using metapelite thermobarometry and calcite–graphite isotope thermometry show a continuous increase in pressure and temperature within the inverted Barrovian metamorphic sequence. Hence, peak PT conditions estimated in individual thrust sheets are interpreted as a metamorphic field gradient developed during continental underthrusting (Štípská et al., 2000). An important question arises as to whether we can attribute the microstructure Type 1 to this tectonic episode. Our microstructural study showed that Type 1 microstructure is preserved in S1 fabric in all tectonic units and that it shows a systematic increase in grain size, which correlates well with coarsening of minerals in surrounding metasediments and with increasing metamorphic grade. Highly asymmetrical grain boundary configurations and measured textures indicate that the mechanism of dislocation creep with grain boundary migration recrystallisation associated with a simple shear deformation was the dominant process during development of Type 1. We suggest that these microstructures originated during an underthrusting event associated with a continuous increase in temperature.

Štípská and Schulmann (1995) suggested that crustal imbrication began in the most metamorphosed and deeply buried IZ unit, which was detached from the underthrust plate and transported upwards in the form of a large crustal nappe. This process of crustal scale foreland imbrication is repeated several times at different depths, so that the Barrovian metamorphic isograds are mechanically inverted. During this period the active thrust plane migrates downwards leading to further deformation of underlying rocks.

We suggest that the deformation associated with this imbrication and successive nappe emplacement is recorded in marbles and expressed by microstructure Type 2 that overprints previous microstructure Type 1 in the Upper

and Lower Nappes. Our study shows a decrease of grain size, increase of intensity and symmetry of grain boundary preferred orientation with respect to Type 1 microstructure. The deformation mechanism of dislocation creep was still operating with a possible minor contribution of grain boundary sliding. The effect of D2 thrusting is the most pronounced in marbles of the Lower Nappe directly underlying a thick orthogneiss body in the footwall of the Upper Nappe. Here, marbles form a continuous 300–400-m-thick layer below the major thrust contact. This layer of mylonitic marbles probably originated due to coalescence of originally smaller marble bodies. The Type 2 microstructure almost completely overprints Type 1 microstructure over the entire width of the marble layer. We suggest that marbles served as a lubricant horizon along which highly competent orthogneiss of the Upper Nappe was thrust. In contrast, in the Upper Nappe the coalescence of marble bodies did not occur during thrusting of the Internal Zone, which correlates well with rather weak development of Type 2 microstructure. This may result from the fact that low competency metasediments of the Internal Zone were thrust over metasediments of the Upper Nappe so that the deformation was more regularly distributed in both units.

The absence of post-kinematic recrystallisation and annealing in the marbles from the Upper Nappe and Internal Zone raises the question of how such microstructures and textures are preserved. In the previously described tectonic setting, thermo-mechanical conditions associated with the process of underthrusting probably continued to exist while the first nappe was being detached. This suggests that microstructures recording dynamic conditions of deformation were not entirely reworked by static recrystallisation. Therefore, at the grain-scale of the continuously strained marbles, the intra-crystalline strain energy remained an important driving force in competition with grain surface energy, so that the original microstructure and textures were preserved.

In the Parautochthon the D2 thrusting event is connected with development of Type 3 microstructure and rather strong reworking of S1 fabrics and of Type 1 microstructure. The Type 3 microstructure is also developed within D3 extensional zones crosscutting marbles and surrounding metapelites of the Upper Nappe and the Internal Zone. This deformation microstructure is marked by strong grain size reduction, development of sub-equant grains characterised by weak textures suggesting a high contribution of diffusion creep.

In conclusion, the thrust related microstructures show a higher contribution of dislocation creep in deep crustal levels, whereas diffusion creep becomes important in shallow ones. The diffusion creep via grain boundary sliding operates also in syn-convergent extensional shear zones at shallow crustal levels.

7.2. Stress and strain rate in underthrusting history

Relationships between strain rate, differential stress, temperature and grain size were tested on naturally deformed quartz mylonites by Werling (1992). Following his approach, independent strain rate estimates were carried out on the marbles studied. We have plotted the calculated flow stress values of Type 1 microstructure based on grain boundary migration paleopiezometry (Rutter, 1995) and peak temperature estimates from individual units on a log differential stress/temperature diagram (Fig. 10a). These data show a decrease of flow stress with increasing metamorphic temperature estimates, which is in agreement with experimental studies suggesting decreasing strength of marbles with increasing temperature (e.g. Schmid, 1982). The flow stress data were further compared with strain rate isolines calculated from experimental flow laws (Heard and Raleigh, 1972; Schmid et al., 1980) and projected into the same diagram. Flow stress values estimated from measured

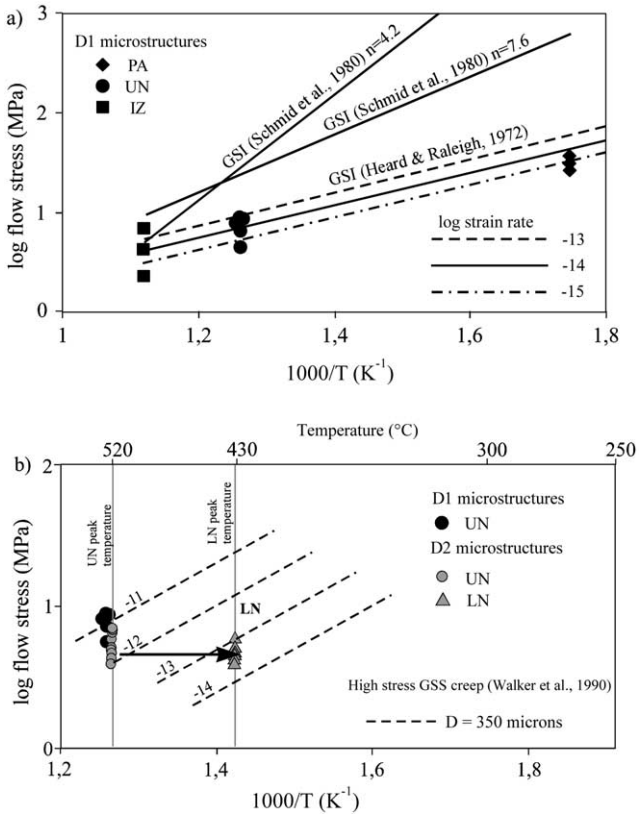

Fig. 10. Homologous temperature versus log differential stress diagrams showing comparisons of the flow stresses calculated from experimental flow laws and different paleopiezometric equations. (a) Underthrusting (D1): points are plotted according to measured average grain size of the marbles from the PA, UN and IZ and corresponding estimated peak temperatures. Squares—Internal Zone; triangles—Upper Nappe; diamonds—Parautochton. Flow stress calculated using GBM paleopiezometer (Rutter, 1995) and peak temperature estimates compared with stress curves of experimental flow laws calculated at constant strain rates (Heard and Raleigh 1972; Schmid et al., 1980). (b) Nappe stacking (D2): flow stress calculated using SGR paleopiezometer after Rutter (1995) compared with stress curves calculated using the flow law for the high-stress grain size sensitive regime (HS-GSS) of Walker et al. (1990). Arrows indicate a temperature interval where the Type 2 microstructure in the UN could be developed during nappe stacking.

grain size of microstructures of Type 1 fit remarkably well with flow law of grain size insensitive creep of Heard and Raleigh (1972). The range of strain rates varies from lower greenschist to amphibolite facies conditions around 10^{-14} s^{-1} (Fig. 10a) that is, in a range typical of continental deformation (Carter and Tsenn, 1987).

The presented peak PT data for each unit are compatible with results of 2D numerical thermal models of continental underthrusting at an angle of 30° with typical velocity of underthrusting of 10–15 mm year^{-1} and uniform erosion rate of 1 mm year^{-1} (Henry et al., 1997). In such a model the deformation of subducted sedimentary cover containing marbles can be approximated by homogeneous simple shear of viscous medium 5 km thick transported downwards on top of basement. Applying the parameter values described above, the strain rate for simple shear deformation in layer of sediments correspond to 6.34×10^{-14} s^{-1}. The values of calculated principal elongation are $e_1 = 1.5$ (D parameter of Ramsay and Huber (1983) = 2.8) at 5 km depth (Parautochthon) and $e_1 = 11$ ($D = 17$) at 30 km depth (Internal Zone). These values of finite strain correspond well with values commonly reported from crustal rocks (Pfiffner and Ramsay, 1982). Strain rate value calculated in such a way is close to that estimated in our microstructural study (Fig. 10a). This coincidence may be interpreted in terms of homogeneous deformation of marbles and surrounding sediments during underthrusting.

7.3. Stress and strain rate during thrust sheets emplacement

In order to estimate strain rates in marbles it is important to discuss the range of possible temperatures associated with the imbrication event and the development of Type 2 and 3 microstructures in individual units. We showed above that the microstructure Type 2 in the marbles of the Upper and the Lower Nappes and the microstructure Type 3 in the Parautochthon originated during thrusting. According to the tectonic model of Štípská and Schulmann (1995) and Štípská et al. (2000) the thermal conditions associated with deformation of marbles in individual units should be close to, or lower than, peak temperatures recorded in an actively deforming footwall unit.

In the Upper and Lower Nappes the flow stress estimates were calculated using both grain boundary migration and sub-grain rotation recrystallisation paleopiezometers for reasons discussed in the section related to paleopiezometry. The estimated stress values calculated by the grain boundary migration paleopiezometer for microstructure Type 2 show an increase of flow stress during thrusting with respect to Type 1 microstructure. However, we assume that the marbles, mainly in the Lower Nappe behaved as a weak lubricating layer during D2 thrusting and therefore the decrease of flow stress is consistent with this assumption. Indeed, such a decrease in flow stress is obtained applying the sub-grain rotation paleopiezometer (Fig. 9). The decrease of flow stress associated with the thrusting event is even more pronounced in the Parautochthon D2 shear zones where Type 3 microstructure is developed. This microstructure shows a high contribution of diffusion creep, which precludes the use of paleopiezometric methods but indicates a significant decrease of flow stress (Schmid et al., 1981) with respect to Type 1 microstructure. We conclude that the characteristic feature of D2 thrust related microstructures Type 2 and 3 in marbles is the grain size reduction, which is connected with important weakening of these lubricant layers mainly in the Lower Nappe and the Parautochthon.

The stress values were plotted on a log differential stress–temperature diagram using peak temperature conditions of 520 and 430 °C for the Upper and the Lower Nappe, respectively (Fig. 10b). We have interpreted Type 2 microstructures developed in the Upper and the Lower Nappe as being similar to those described in the high stress grain-size sensitive regime of Walker et al. (1990). So, strain rate isolines calculated using the flow law of high-stress grain size sensitive regime (HS-GSS) of Walker et al. (1990) for constant average grain size of 350 microns were compared with paleopiezometric estimates and plotted on the same diagram (Fig. 10b). An estimated strain rate of around 10^{-13} s^{-1} shows that development of D2 thrust related microstructures Type 2 in the Lower Nappe is connected with an increase in strain rate with respect to the D1 event. The decrease in recrystallised grain size connected with development of Type 2 microstructure in the Upper Nappe may be connected either with a dramatic increase in strain rate up to 10^{-12} s^{-1} at a peak temperature of 520 °C or by a strain rate increase of up to 10^{-13} s^{-1} at a temperature lower than a peak of 430 °C during the thrusting (Fig. 10b).

Similar strain rates of 1.06×10^{-12} and 8×10^{-13} s^{-1} can be calculated assuming homogeneous simple shear operating over zones of 300 and 400 m wide, respectively, which corresponds to the width of the marble layer at the top of the Lower Nappe. We assumed a similar thrusting angle of 30° and velocity of thrusting of 10 mm year^{-1} as for the previous calculations. The calculated principal elongation equals $e_1 = 32$ ($D = 47$) and $e_1 = 24$ ($D = 35$) for 300 and 400-m-wide zones, respectively, during 1 Ma of thrusting. Such finite strain intensities exceed realistic values recorded in nature, which means that the marbles have to be deformed for periods shorter than 1 Ma for the geometry defined above. Consequently, our strain rate estimates suggest that the microstructure Type 2 associated with thrusting was developed during episodic short-lived events for the marble layer of the Lower Nappe. Even if we cannot make similar calculations for marbles of the Upper Nappe and the Parautochthon, similar episodic thrusting events are likely.

8. Conclusions

The inverted metamorphic sequence shows three types of

microstructures in deformed marbles associated with continental underthrusting, imbrication and stacking of the nappe sequence and extensional syn-convergent collapse. Detailed microstructural and textural work combined with the existing thermobarometrical database allows us to correlate microstructural types with tectonic events and to discuss the possible significance of stress and strain rate estimates.

The recrystallised grain size of Type 1 microstructure related to D1 continental underthrusting increases with increasing metamorphic grade, and the highly asymmetrical grain boundary configuration ($65° < \Delta\alpha < 80°$) indicate grain boundary migration recrystallisation mechanisms developed during a simple shear type underthrusting regime. Textural analysis shows increasing intensity of lattice preferred orientation with increasing temperature. Paleopiezometric calculations show a decrease of flow stress with increasing metamorphic temperature and strain rate estimates vary from lower greenschist to amphibolite facies conditions slightly around $10^{-14}\,s^{-1}$.

D2 thrust related microstructures Type 2 and 3 in marbles are marked by grain size reduction, which is connected with important weakening (Rutter and Brodie, 1988) of these lubricant layers mainly in the Lower Nappe and Parautochthon. The Type 2 microstructure develops during active thrusting of Internal Zone and Upper Nappe (amphibolite facies units) and is characterised by an increase in intensity and symmetry of grain boundary configuration with respect to Type 1 microstructure. Microstructural and textural studies indicate dislocation creep with a possible (and subordinate) contribution of grain boundary sliding. Paleopiezometric calculations show a decrease in flow stress with respect to the Type 1 microstructure when sub-grain rotation paleopiezometer is applied. A strain rate between 10^{-12} and $10^{-13}\,s^{-1}$ was estimated for the development of D2 thrust related microstructures of Type 2 in the Lower Nappe and the Upper Nappe.

Type 3 microstructure is developed in D2 shear zones in the Parautochthon. This microstructure shows a high contribution of diffusion creep that precludes the use of paleopiezometric methods but indicates low values of flow stress and significant weakening of marble layers.

The general feature of the studied area is the localisation of deformation into marbles during thrusting in low metamorphic grades while in higher grades marbles are not exploited as lubricating layers.

Acknowledgements

This work was supported by the Grant Agency of the Czech Republic (grant no. 42-201204) and by a Ministry of Education grant (no. 2431 3005). Ondrej Lexa from our Institute is thanked for software support. Comments of annonymous reviewer, Jeff Amato and Florian Heidelbach are gratefully acknowledged.

References

Ave Lallemand, H.G., Carter, N.L., 1971. Pressure dependence of quartz deformation lamellae orientations. American Journal of Science 270, 218–235.

Burkhard, M., 1990. Ductile deformation mechanisms in micritic limestones naturally deformed at low temperatures (150–350 °C). In: Knipe, R.J., Rutter, E.H. (Eds.), Deformation Mechanisms, Rheology and Tectonics. Geological Society Special Publication 54, pp. 241–257.

Burkhard, M., 1993. Calcite twins, their geometry, appearance and significance as stress-strain markers and indicators of tectonic regime: a review. Journal of Structural Geology 15 (3–5), 351–368.

Carter, N.L., Tsenn, M.C., 1987. Flow properties of continental litosphere. Tectonophysics 136, 27–63.

Casey, M., 1981. Numerical analysis of X-ray texture data: an implementation FORTRAN allowing triclinic or axial specimen symmetry and most crystal symmetries. In: Lister, G.S., Weber, H.-J.B.K., Zwart, H.J. (Eds.), The Effect of Deformation on Rocks. Tectonophysics 78, pp. 51–64.

Casey, M., Kunze, K., Olgaard, D.L., 1998. Texture of Solenhofen limestone deformed to high strains in torsion. Journal of Structural Geology 20 (2/3), 255–267.

Chlupáč, I., 1994. Facies and biogeographic relationships in Devonian of the Bohemian massif. Cour. Forsch.–Senckenberg 169, 299–317.

Čížek, J., 1985. Isotopic composition of C in graphite deposits of the Bohemian Massif. Unpublished MSc thesis, Charles University (in Czech).

Covey-Crump, S.J., Rutter, E.H., 1989. Thermally induced grain growth of calcite marbles on Naxos island, Greece. Contributions to Mineralogy and Petrology 101 (1), 69–86.

Dietrich, D., Song, H., 1984. Calcite fabrics in a natural shear environment, the Helvetic nappes of western Switzerland. Journal of Structural Geology 6 (1/2), 19–32.

Dudek, A., 1980. The crystalline basement block of the Outher Carpathians in Moravia–Brunovistulicum. Rozpr. čs. Akad. Věd 90 (8), 85.

Exner, H.E., 1972. Analysis of grain and particle size distributions in metallic materials. International Metalurgical Reviews 17, 25–42.

Fritz, H., Dallmeyer, R.D., Neubauer, F., Urban, M., 1994. Thick-skinned versus thin-skinned thrusting: mechanism of the formation of inverted metamorphic sections in the SE Bohemian Massif. Mineralogii a Geologii 39 (1), 33–34.

Heard, H.C., Raleigh, C.B., 1972. Steady-state flow in marble at 500 to 800 °C. Geological Society of America Bulletin 83, 935–956.

Henry, P., LePichon, X., Goffe, B., 1997. Kinematic, thermal and petrological model of the Himalayas: constraints related to metamorphism within the underthrust Indian crust and topographic elevation. Tectonophysics 273 (1–2), 31–56.

Johan, V., Autran, A., Ledru, P., Lardeaux, J.-M., Melka, R., 1990. Discovery of relics of a high-pressure metamorphism at the base of the Moldanubian nappe complex. In: Proc. Int. Conf. on Paleozoic Orogens in Central Europe. IGCP 233, Göttingen, Germany.

Kern, H., Wenk, H.R., 1983. Calcite texture development in experimentally induced ductile shear zone. Contributions to Mineralogy and Petrology 83, 231–236.

Knipe, R.J., 1989. Deformation mechanisms—recognition from natural tectonites. Journal of Structural Geology 11, 127–146.

Knipe, R.J., 1990. Microstructural analysis and tectonic evolution in thrust systems: examples from the Assynt region of the Moine thrust zone, Scotland. In: Barber, D.J., Meredith, P.G. (Eds.). Deformation Processes in Minerals, Ceramics and Rocks. Unwin Hyman, London, pp. 228–261.

Kohlstedt, D.L., Weathers, M.S., 1980. Deformation induced microstructures, paleopiezometers and differential stresses in deeply eroded fault zones. Journal of Geophysical Research 85 (B11), 6269–6285.

Mercier, J.-C.C., Anderson, D.A., Carter, N.L., 1977. Stress in the

lithosphere: inferences from steady state flow of rock. Pure and Applied Geophysics 115, 199–226.

Panozzo, R., 1984. Two-dimensional strain from the orientation of lines in a plane. Journal of Structural Geology 6, 215–221.

Pfiffner, O.A., Ramsay, J.G., 1982. Constraints on geological strain rates: arguments from finite strain states of naturally deformed rocks. Journal of Geophysical Research 87, 311–321.

Pitra, P., Guiraud, M., 1996. Probable anticlockwise P–T evolution in extending crust: Hlinsko region, Bohemian massif. Journal of Metamorphic Geology 14, 49–60.

Poirier, J.P., 1985. Creep of Crystals. High Temperature Deformation Processes in Metals, Ceramics and Minerals. Cambridge University Press.

Ramsay, J.G., Huber, M.I., 1983. The Techniques of Modern Structural Analysis. Volume 1: Strain Analysis. Academic Press, London.

Rutter, E.H., 1995. Experimental study of the influence of stress, temperature, and strain on the dynamic recrystallization of Carrara marble. Journal of Geophysical Research 100 (B12), 24,651–24,663.

Rutter, E.H., Brodie, K.H., 1988. The role of tectonic grain size reduction in the rheological stratification of the lithosphere. Geologische Rundschau 77 (1), 295–308.

Schmid, S.M., 1982. Microfabric studies as indicators of deformation mechanisms and flow laws operative in mountain building. In: Hsu, K. (Ed.). Mountain Building Processes, pp. 95–110.

Schmid, S.M., Paterson, M.S., Boland, J.N., 1980. High temperature flow and dynamic recrystallization in Carrara marble. Tectonophysics 65, 245–280.

Schmid, S.M., Casey, M., Starkey, J., 1981. The microfabric of calcite tectonites from the Helvetic Nappes. In: McClay, K.R., Price, N.J. (Eds.). Thrust and Nappe Tectonics. The Geological Society of London, pp. 151–158.

Schmid, S.M., Panozzo, R., Bauer, S., 1987. Simple shear experiments on calcite rocks: rheology and microfabric. Journal of Structural Geology 9 (5/6), 747–778.

Schulmann, K., Ledru, P., Autran, A., Melka, R., Lardeaux, J.M., Urban, M., Lobkovicz, M., 1991. Evolution of nappes in the eastern margin of the Bohemian Massif: a kinematic interpretation. Geologische Rundschau 80 (1), 73–92.

Schulmann, K., Melka, R., Lobkowicz, M., Ledru, P., Lardeaux, J.-M., Autran, A., 1994. Contrasting styles of deformation during progressive nappe stacking at the southeastern margin of the Bohemian Massif (Thaya Dome). Journal of Structural Geology 16 (6), 355–370.

Suess, F.E., 1912. Die Moravischen Fenster und ihre Beyiehong yum Grundgebirge des Hohen Gesenks. Denkschr. K. Akad. Wiss. Wien 88, 541–631.

Suess, F.E., 1926. Intrusionstektonik und Wandertektonik im variszischen Grundgebirgen, Berlin.

Štípská, P., Schulmann, K., 1995. Inverted metamorphic zonation in a basement-derived nappe sequence, eastern margin of the Bohemian Massif. Geological Journal 30, 385–413.

Štípská, P., Schulmann, K., Höck, V., 2000. Complex metamorphic zonation of the Thaya dome: result of buckling and gravitational collapse of an imbricated nappe sequence. In: Cosgrowe, J.W., Ameen, M.S. (Eds.), Forced Folds and Fractures. The Geological Society of London, Special Publication 169, pp. 197–211.

Štoudová, S. 1998. Contrasting PT and structural evolution of granulite megaboudine and surrounding metapelites: Policka crystalline unit, eastern margin of the Bohemian Massif. Unpublished MSc thesis, Charles University, Prague (in Czech).

Thompson, A.B., Ridley, J.R., 1987. Pressure–temperature–time (P–T–t) histories of orogenic belts. Philosophical Translations of the Royal Society, London A 321, 27–45.

Tichý, M., 1992. Inverse metamorphism in the northern flank of the Svratka dome, Unpublished MSc thesis, Charles University, Prague (in Czech).

Ulrich, S., 2000. Deformation microstructures and comparative rheology of marble and quartzite in natural strain and metamorphic gradient. Unpublished PhD thesis, Charles University.

Van Der Pluijm, B.A., 1991. Marble mylonites in the Bancroft shear zone, Ontario, Canada: microstructures and deformation mechanisms. Journal of Structural Geology 13 (10), 1125–1135.

Walker, A.N., Rutter, E.H., Brodie, K.H., 1990. Experimental study of grain-size sensitive flow of syntetic, hot-pressed calcite rocks. In: Knipe, R.J., Rutter, E.H. (Eds.), Deformation Mechanisms, Rheology and Tectonics. Geological Society Special Publication 54, pp. 259–284.

Weber, R., 1996. Metamorphism of rock of the Bíly potok group. Unpublished MSc thesis, Masaryk University, Brno (in Czech).

Werling, E. 1992. Tonale-, pejo- und judicarien-linie: kinematik, mikrostrukturen und metamorphose von tektoniten aus raumlich interferierenden aber verschiedenaltrigen verwerfungszonen, ETH.

White, S., 1976. The effect of strain on the microstructures, fabrics and deformation mechanisms in quartzites. Philosophical Translations of the Royal Society, London A 283, 69–86.